Analytica Chimica Acta 748 (2012) 81–88

Contents lists available at SciVerse ScienceDirect

Analytica Chimica Acta

journal homepage: www.elsevier.com/locate/aca

A rational design of the multiwalled carbon nanotube–7,7,8,8-tetracyanoquinodimethan sensor for sensitive detection of acetylcholinesterase inhibitors

Lucian Rotariu[a,b], Lucian-Gabriel Zamfir[a,b], Camelia Bala[a,b,*]

[a] Department of Analytical Chemistry, University of Bucharest, 4-12 Regina Elisabeta Blvd., 030018 Bucharest, Romania
[b] LaborQ, University of Bucharest, 4-12 Regina Elisabeta Blvd., 030018 Bucharest, Romania

HIGHLIGHTS

- A new concept based on the interaction between MWCNTs and TCNQ was developed.
- Synergistic effect of MWCNT and TCNQ allow thiocholine detection with high sensitivity.
- Low detection limit of 7 ppt for paraoxon-methyl and 0.1 ppb for chlorpyrifos, respectively.

GRAPHICAL ABSTRACT

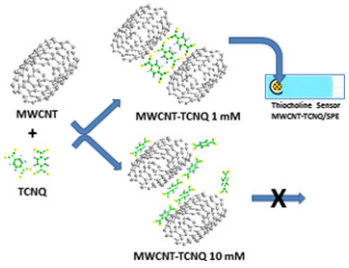

ARTICLE INFO

Article history:
Received 16 March 2012
Received in revised form 13 August 2012
Accepted 28 August 2012
Available online 4 September 2012

Keywords:
Carbon nanotube
TCNQ
Acetylcholinesterase
Supramolecular arrangement
Screen printed electrode
Biosensor

ABSTRACT

A new, simple and effective amperometric acetylcholinesterase biosensor was developed using screen-printed carbon electrodes modified with carbon nanotubes (MWCNTs)–7,7,8,8-tetracyanoquinodimethane (TCNQ). The design of the biosensor was based on the supramolecular arrangement resulted from the interaction of MWCNTs and TCNQ. This arrangement was confirmed by spectroscopic and electrochemical techniques. Two different supramolecular arrangements were proposed based on different MWCNTs:TCNQ ratios. The synergistic effect of MWCNTs and TCNQ was, for the first time, exploited for detection of thiocholine at low potential with high sensitivity. The biosensor developed by immobilization of acetylcholinesterase (AChE) in sol–gel allowed the detection of two reference AChE inhibitors, paraoxon-methyl and chlorpyrifos with detection limits of 30 pM (7 ppt) and 0.4 nM (0.1 ppb), respectively. Efficient enzyme reactivation was obtained by using obidoxime.

1. Introduction

Pesticide residues represent a major concern due to their high toxicity toward humans and animals and therefore a fast detection at low concentrations is of great importance [1]. To solve this problem several methods have already been proposed including electrochemical biosensors [2,3]. The biosensors for pesticide detection have the advantage of a high sensitivity and could be easily integrated in portable devices offering the possibility of on site measurements. The poisoning effect of organophosphate and carbamate pesticides is based on the inhibition of the acetylcholinesterase (AChE) by phosphorylation or carbamoylation of the active site [2]. The enzymatically generated thiocholine (TCh) is an electro-active compound, which can serve as an indicator to reflect the inhibition effect of pesticides. On unmodified carbon-based electrodes, TCh is oxidized at a potential as high as +700 mV *vs.* Ag/AgCl. Such a high value leads to a high background current and can cause interferences from other electroactive species

* Corresponding author at: Department of Analytical Chemistry, University of Bucharest, 4-12 Regina Elisabeta Blvd., 030018 Bucharest, Romania.
Tel.: +40 21 4104888; fax: +40 21 4104888.
E-mail address: camelia.bala@g.unibuc.ro (C. Bala).

0003-2670/$ – see front matter © 2012 Elsevier B.V. All rights reserved.
http://dx.doi.org/10.1016/j.aca.2012.08.045

present in the sample. In order to reduce the oxidation potential of TCh, various mediators were already reported in the literature, such as potassium ferrocyanide [4], cobalt phthalocyanine (CoPC) [5], Prussian blue [6], cobalt hexacyanoferrate [7]. Highly conductive nanomaterials such as carbon nanotubes (CNTs), were also reported to decrease the TCh oxidation potential [8,9]. The use of immobilized multi-walled carbon nanotubes (MWCNTs) and AChE in polyelectrolyte multilayers has reduced the working potential to +150 mV *vs.* Ag/AgCl [8]. Also, mixtures of CNTs and imidazolium-based ionic liquids allowed detection of TCh at +50 mV *vs.* Ag/AgCl, with high sensitivity and detection limits between 0.05 and 0.08 mM TCh [10]. The sensors were further used for the detection of chlorpyrifos with a detection limit of 4 nM [11].

The discovery of the highly conducting 7,7,8,8-tetracyanoquinodimethane (TCNQ) paramagnetic salt constituted an important advancement in the development of biosensors based on AChE inhibitions [12]. Thus, several groups have used TCNQ together with various types of carbonaceous materials obtaining a significant signal enhancement for the oxidation of TCh compared with the unmodified electrodes [13–15]. However, studies on CNTs and TCNQ were scarcely reported, and they refer only to spectroscopic characterizations [12,16].

The CNTs modification with TCNQ can be made in different ways. Both doping and deposition can be envisaged as possible routes. The main advantage of noncovalent adsorption (physisorption) over covalent one (chemisorption) is that the former may modify the electronic properties of CNTs in a sizable way. However, it does not drastically change its atomic structure. Noncovalent adsorption is, in principle, easily reversible.

Since there are no chemical bonds between the adsorbed molecule and the CNTs, the chemical and mechanical properties of CNTs are only weakly perturbed [17]. Not only density functional theory and semi-empirical methods [18] but also *Ab initio* calculations demonstrated that bridge configurations represent the energetically most favorable physisorbed structures. The TCNQ–CNTs binding energy increases as a function of the nanotube radius. In accordance to this model, encapsulated systems exhibited similar binding energies [19]. The electronic charge transfers always occurs from the CNTs toward the molecule, being proportional to the TCNQ–CNTs binding energy [17]. Similar conclusions were achieved using density functional theory and semi-empirical methods [18]. Raman investigations provided evidence for this type of interaction [12]. X-ray photoelectron spectroscopy and near-infrared data have also been reported for the same purpose [16].

The biosensor analytical performance could be dramatically affected by the AChE immobilization procedure. Results using various immobilization methods: direct adsorption [20], cross-linking on chitosan–MWCNTs composite *via* glutaraldeyde [21] mixing the enzyme in polymers [22] or MWCNTs/sol–gel route [23] confirmed this fact.

This study aimed to investigate MWCNTs–TCNQ as electrode materials for the (bio)sensors development. Spectroscopic investigations were carried out in order to identify the interactions between TCNQ and MWCNTs. Electrochemical experiments allowed us to characterize and optimize the TCh sensor. In order to stabilize the catalytic activity of the AChE and prevents enzyme leaching a sol–gel network was selected for immobilization. Paraoxon-methyl and chlorpyrifos were selected as reference pesticide for testing the biosensor.

2. Experimental

2.1. Materials and reagents

Acetylcholinesterase (from electric eel, 425.94 IU mg^{-1}) acetylthiocholine chloride (ATCh, purity ≥ 99%), multiwalled carbon nanotubes (purity ≥ 95%, outside diameter = 40–60 nm, inside diameter = 5–10 nm, length = 0.5–500 μm), potassium ferricyanide ($K_3[Fe(CN)_6]$), potassium ferrocyanide ($K_4[Fe(CN)_6]$), potassium chloride, sodium phosphate dibasic, potassium phosphate monobasic, 7,7,8,8-tetracyanoquinodimethane (TCNQ), Nafion (∼5% in a mixture of lower aliphatic alcohols and water), obidoxime (1,1′-[oxybis(methylene)]bis 4-[(E)-(hydroxyimino)methyl]pyridinium), acetonitrile (ACN, purity ≥ 99.9%), tetramethoxysilane (TMOS), methyltrimethoxysilane (MTMOS), polyethylene glycol (PEG600) were purchased from Sigma–Aldrich. Paraoxon-methyl (O,O-dimethyl O-(4-nitrophenyl) phosphate, purity ≥ 96%) was purchased from Fluka and chlorpyrifos (O,O-diethyl-O-3,5,6-trichloro-2-pyridyl phosphorothioate, purity ≥ 99.9%) was purchased from Riedel-de Haën. The phosphate buffer (PBS) solution 0.1 M, containing 0.1 M KCl, and the 0.1 M ATCh stock solution were prepared in ultrapure water. The AChE stock solution (66 IU mL^{-1}) was prepared in 0.1 M PBS, pH 8. The paraoxon-methyl and chlorpyrifos dilutions were each prepared in ultrapure water from a 10^{-4} M stock solution prepared in acetonitrile. The ATCh and pesticide dilutions were prepared directly from stock solutions prior to their use in measurements.

2.2. Instruments

Cyclic voltammetry, chronoamperometry measurements and electrochemical impedance spectroscopy (EIS) were carried out using a potentiostat AUTOLAB PGSTAT-12 (Eco Chemie, Utrecht, The Netherlands) and the software used to gather data was GPES 4.9. The screen-printed electrodes (SPE, Dropsens 110) consist of a three-electrode system having a carbon working electrode (4 mm diameter), a silver pseudo-reference electrode and a carbon counter electrode. Before each experiment a film of silver chloride on the silver pseudo-reference electrode was electrochemically deposited from a phosphate buffer solution in the presence of 0.1 M KCl, according to procedure reported by Arduini [24]. All experiments were carried out at room temperature (22 °C), using a 10 mL cell. Raman spectra were recorded using a Horiba Jobin Yvon-Labram HR spectrophotometer. DR-UV–vis spectra were recorded with Analytik Jena Specord 250 spectrophotometer. Elemental analysis was performed with EuroEA 3000 elemental analyzer (Euro Vector Instruments, Italy).

2.3. Modification of the screen-printed electrodes

Before any modification the SPEs were electrochemically pretreated by application of a potential of 1200 mV in sulfuric acid 0.1 M, for 2 min. Three types of screen-printed modified electrodes were prepared: SPEs modified with MWCNTs (MWCNTs/SPE), SPEs modified with TCNQ (TCNQ/SPE) and SPEs modified with MWCNTs–TCNQ (MWCNTs–TCNQ/SPE). For TCNQ/SPE, a 1 mM TCNQ solution was prepared in acetonitrile (solution A). In the case of MWCNTs/SPE and MWCNTs–TCNQ/SPE, 2 mg of MWCNTs were suspended in 100 μL acetonitrile (solution B), respectively in 100 μL TCNQ 1 mM (solution C), by sonication for 45 min in a 0.5 mL tube. A volume of 5 μL solution A, B or C were mixed with 45 μL ACN then, 5 μL from each mixture were casted on the working electrodes and left overnight to dry at 4 °C in a desiccator. TCNQ loading was 0.8 μg cm^{-2} for TCNQ/SPE and MWCNTs–TCNQ/SPE. In order to avoid the TCNQ leaching, Nafion was used only for preparation of TCh sensors. Modified electrodes with Nafion were prepared in a similar manner by replacing the ACN with Nafion (5%).

2.4. Preparation of the biosensors

The sol–gel matrix for AChE immobilization was prepared according to a method reported earlier [11] by mixing 100 μL TMOS

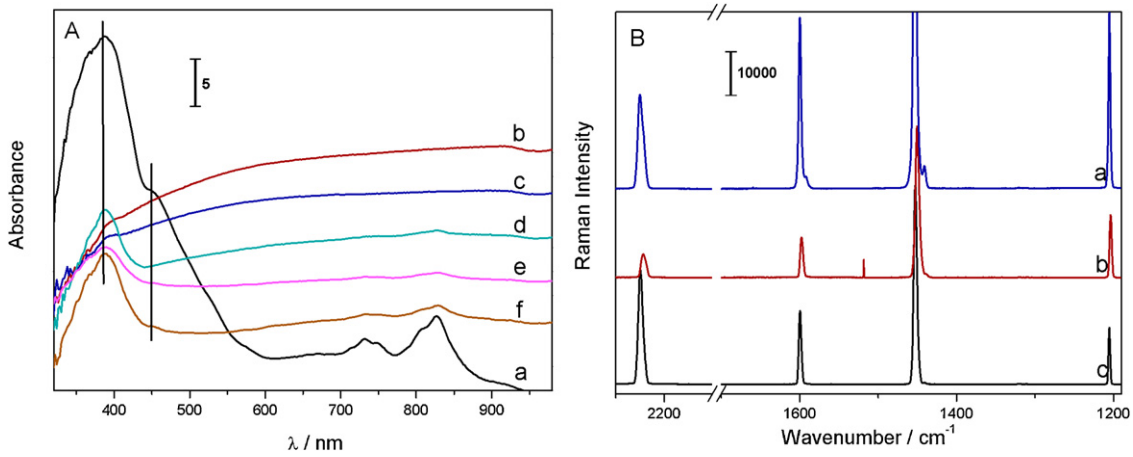

Fig. 1. (A) DR-UV–vis spectra of TCNQ (a), MWCNTs (b), MWCNTs–TCNQ 1 mM (c), MWCNTs–TCNQ 10 mM (d), MWCNTs–TCNQ 100 mM (e), and MWCNTs–TCNQ 200 mM (f). (B) Raman spectra of TCNQ (a), MWCNTs–TCNQ 100 mM (b), and MWCNTs–TCNQ 200 mM (c).

and 100 μL MTMOS with 400 μL of ultrapure water, 440 μL of HCl 1 mM and 40 μL PEG600. The AChE solution was mixed with sol–gel in a ratio of 50:50 (v) and 5 μL of this mixture was dropped on the SPEs. 17 m IU AChE was immobilized on the surface of the electrode according to previously optimized protocol [11]. The enzymatic activity was determined by the spectrophotometric Ellman method. The biosensor was left to dry 3–4 h at 4 °C and stored in phosphate buffer pH = 8 at 4 °C.

2.5. Amperometric and inhibition measurements

The biosensor was placed into 5 mL PBS solution and a potential of +150 mV was applied. After stabilization of the current, the acetylthiocholine solution was injected and the steady-state current was recorded. Between measurements the biosensor was washed with distilled water and PBS. For the inhibition measurement, the AChE biosensor was incubated with pesticide solution and the TCh oxidation current was measured at the same substrate concentration.

The degree of inhibition (*I*%) was calculated according to the formula:

$$\text{Inhibition } (\%) = \frac{i_0 - i_I}{i_0} \times 100 \quad (1)$$

where i_0 and i_I are the currents of thiocholine oxidation measured prior to and after the contact of the biosensor with inhibitor, respectively.

After the biosensor was exposed to the pesticide solution a regeneration step was performed by immersion in a 5 mM obidoxime solution. The regeneration degree was estimated as follow:

$$\text{Regeneration } (\%) = \frac{i_R - i_I}{i_0 - i_I} \times 100 \quad (2)$$

where i_R is the current recorded after reactivation with obidoxime, i_0, i_I are the currents recorded without and with pesticide inhibition, respectively.

The biosensor was further washed twice with ultrapure water and then with PBS to completely remove the obidoxime from the biocatalytical layer.

2.6. DR-UV–vis and Raman measurements

The DR-UV–vis and Raman spectra for pure TCNQ powder and mixtures of MWCNTs and TCNQ 1, 10, 100 and 200 mM were recorded. Raman spectra were recorded at room temperature under 688 nm excitation wavelength. Each mixture was prepared as it was described in Section 2.3. Before analysis the mixtures were left to dry overnight at room temperature in a desiccator. DR-UV–vis spectra were recorded using the solid substances mixed with silica.

3. Results and discussion

3.1. Spectroscopic characterization

The TCNQ DR-UV–vis spectrum exhibits absorption peaks at 388 nm attributed to the neutral TCNQ molecule and at 454, 732, 748 and 826 nm, with a lower intensity, attributed to the radical anion ($TCNQ^{\bullet -}$) (Fig. 1A) [25]. The intensity of the bands assigned to the radical ion species is very low in the absence of structures that can allow an electron transfer. Spectra previously reported in acetonitrile also present three absorption bands with maximum at 420, 745 and 840 nm [25]. A very specific characteristic of the MWCNTs–TCNQ 1 mM spectrum is the fact that the band from 454 nm assigned to the radical ion state disappears. This is the result of direct interaction between the CN groups and the aromatic nucleus of CNTs. Consequently this entitles us to assert the formation of the supramolecular arrangement MWCNTs–TCNQ. The peak from 388 nm is also shifted to 393 nm indicating a modification of the neutral form of the mediator due to the interaction with carbon nanotubes.

For the MWCNTs–TCNQ, the band at 454 nm was visible as a weakly prominent shoulder only for 200 mM TCNQ. This indicates that, only at a higher concentration of TCNQ, part of the mediator molecules remained in a native state. The peak from 388 nm reappears for concentration higher than 10 mM indicating that some TCNQ molecules were in a neutral form. These spectra also suggest a limited number of superficial sites that can bond the TCNQ molecules.

The direct interaction of TCNQ with MWCNTs was also confirmed by the Raman spectra (Fig. 1B). Pure TCNQ spectra exhibits stretching vibration modes of $C{=}C_w$ at 1453 cm^{-1}, $C{=}C_r$ at 1599 cm^{-1}, and C≡N at 2225 cm^{-1}, and a C—H bending-vibration mode at 1205 cm^{-1} ("r" stands for ring and "w" for wing). MWCNTs–TCNQ 100 mM shows a shift of the CN vibration at 2221 cm^{-1} that may account for an interaction of the CN groups with the MWCNTs. The shift of the band assigned to the CN group disappears in the case of MWCNTs–TCNQ 200 mM, but a new shift of the bands assigned to $C{=}C_w$ and $C{=}C_r$ has been observed. These can be explained by an electron transfer that occurs between

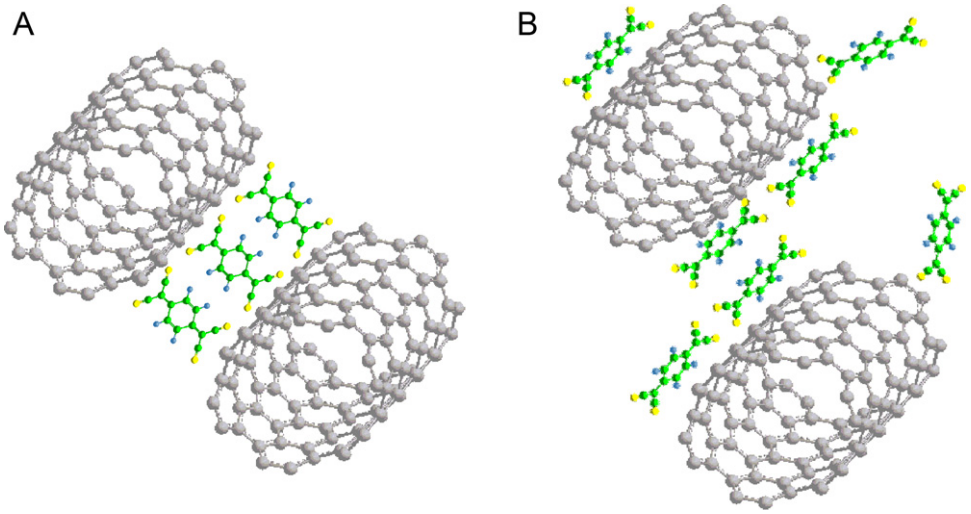

Fig. 2. Supramolecular organization of MWCNTs–TCNQ at (A) low concentration of TCNQ (<1 mM) and (B) high concentration of TCNQ (>10 mM).

MWCNTs and the ionized TCNQ molecules [12]. The shift from 1599 to 1597 cm^{-1} corresponds to an interaction between the ring of the molecule and the CNTs surface. Recent studies by Veiga and Miwa [17] showed through *Ab initio* calculations that TCNQ–CNTs systems can be stabilized by π–π interactions between the adsorbed TCNQ molecule and the carbon rings of the CNTs structure. The claims of Veiga and Miwa are in accordance with our results obtained at high TCNQ concentrations.

Corroborating the spectral results one can conclude that mixing of MWCNTs with TCNQ leads to two different supramolecular configurations as it is suggested in Fig. 2. One can observe that the proposed architecture depends on the TCNQ concentration. The DR-UV–vis and Raman spectroscopy data suggest a different arrangement for low TCNQ concentrations (Fig. 2A) than that for a high TCNQ loading (Fig. 2B). TCNQ molecules have two major roles: they serve as pillars for the MWCNTs and function as electron acceptors for the oxidation of TCh. This property was further exploited in the construction of the TCh sensors.

3.2. Cyclic voltammetry studies

In order to test the effectiveness of the MWCNTs–TCNQ on the oxidation of thiocholine three different types of SPEs were prepared, MWCNTs/SPE, TCNQ/SPE and MWCNTs–TCNQ/SPE were investigated in cyclic voltammetry experiments performed on the potential range from −400 to +800 mV, with a scan rate of 100 mV s^{-1}. Fig. 3 shows the cyclic voltammograms recorded with a solution of TCh 5 mM in PBS for the modified electrodes and bare SPE. One can observe that the oxidation potential for TCh varied depending on the sensor use, decreasing from +700 (bare SPE) to +450 mV (MWCNTs/SPE), +300 mV (TCNQ/SPE) and +150 mV (MWCNTs–TCNQ/SPE). Moreover, one can observe that the remarkable decrease in the necessary overpotential for effective oxidation of TCh on MWCNTs–TCNQ/SPE is accompanied by a significant increase of oxidation current. This was attributed to an enhancement of electron transfer provided by synergistic effect between TCNQ and MWCNTs. The electrocatalytic effect of MWCNTs–TCNQ toward TCh oxidation was further used for improving the AChE based biosensor.

The TCNQ amount in the mixture was optimized with respect to a high and stable electrochemical signal for TCh detection. TCNQ concentration was varied between 0.1 and 50 mM and the amount of MWCNTs was maintained constant. Generally, the current increases with the TCNQ concentration, but a high amount of TCNQ affected the stability of the modified sensor. For MWCNTs–TCNQ/SPEs with TCNQ 50 mM the signal decreased by 20% after 15 scans. On the other hand, two oxidation peaks were observed at higher amount of TCNQ. One could be attributed to the MWCNTs–TCNQ and the other to the free or weakly bound TCNQ. The second peak is similar to the one observed for the TCNQ/SPEs sensor. That proves the existence of an interaction between TCNQ and MWCNTs and the formation of supramolecular structure with different electrochemical properties depending on the concentration of the TCNQ. The stable electrochemical signal recorded for TCh oxidation with MWCNTs–TCNQ/SPE prepared with 1 mM TCNQ could be attributed to the structure presented in Fig. 2A. Increasing the amount of the TCNQ leads to a change of the supramolecular arrangement corresponding to that presented in Fig. 2B. A more or less weak interaction with MWCNTs or even free TCNQ molecules could be found at even higher amounts of mediator added into the mixture. We observed that for concentrations of TCNQ higher than 1 mM, the sensor signal for MWCNTs–TCNQ was not stable. This can be attributed to the fact that at concentrations above 1 mM the TCNQ diffuses into the solution during electrochemical measurements.

The appearance of the second oxidation peak for TCh at higher concentration of TCNQ corresponds to the presence of the native TCNQ molecule revealed by DR-UV–vis spectra. One can conclude

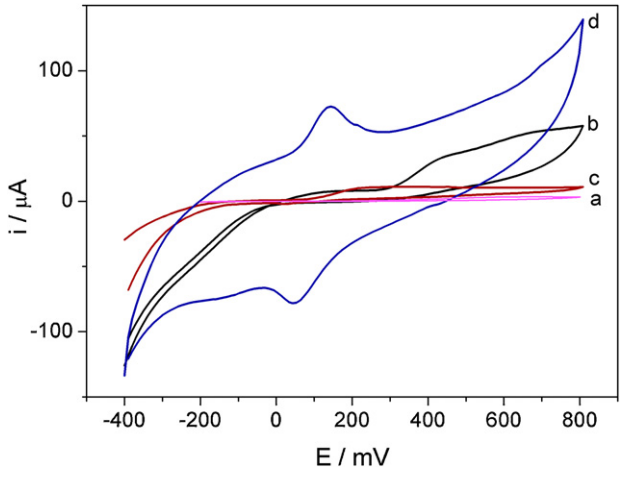

Fig. 3. Cyclic voltammogram of the bare SPE (a), MWCNTs/SPE (b), TCNQ/SPE (c) and MWCNTs–TCNQ/SPE (d) in TCh 5 mM (SR = 100 mV s^{-1}, pH = 8).

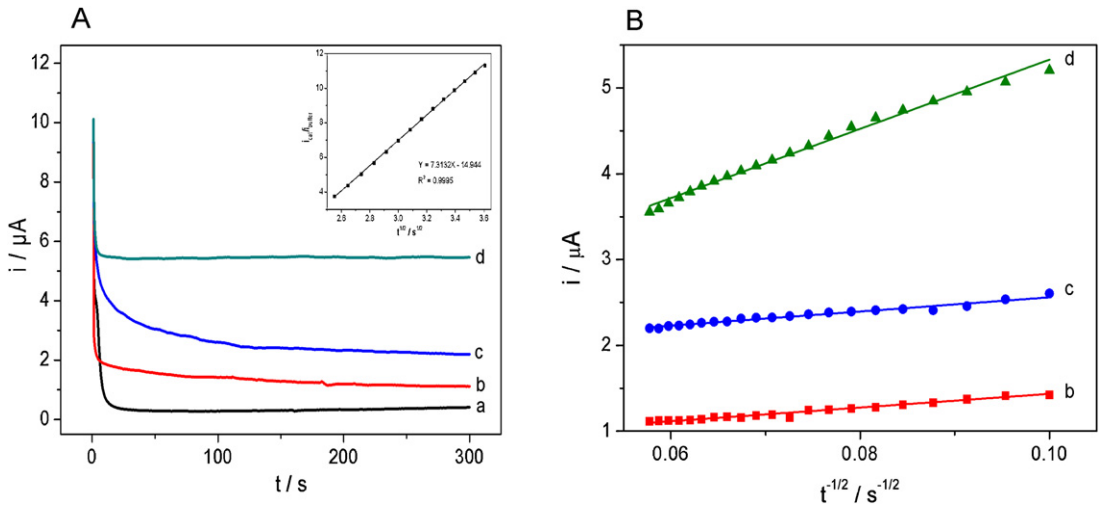

Fig. 4. (A) Chronoamperograms using MWCNTs–TCNQ/SPE electrode in absence (a), and in the presence of TCh 1 mM (b), 2 mM (c), 5 mM (d) (PBS, pH = 8). Inset: plot i_{cat}/i_{buffer} *vs.* $t^{1/2}$ derived from chronoamperometric data for TCh 5 mM (d) and buffer (a). (B) Linear segments of the plot *i vs.* $t^{-1/2}$ for TCh 1 mM (b), 2 mM (c) and 5 mM (d).

that the electrochemical results confirm the spectroscopic data presented in the previous section.

The MWCNT–TCNQ (1 mM) modified electrode gave reproducible values for oxidation peak and current for 15 successive scans. It was considered a good compromise between a high and stable signal and it was used further for all experiments.

The elemental analysis based on nitrogen content was performed in order to study the stability of MWCNT–TCNQ (1 mM). A content of 0.331% N was determined in MWCNT–TCNQ prepared by sonication and evaporation of solvent and 0.314% N in MWCNT–TCNQ prepared by sonication, separation of the solid phase by centrifugation and washing with PBS and distilled water. These results correspond to the TCNQ content of 1.205% and 1.140%, respectively, and confirm a good stability of the MWCNT–TCNQ (1 mM) in the working conditions.

According to the MWCNTs supplier analysis the content in amorphous carbon is around 2%. We do not expect that this carbon will be organized by TCNQ in a way similar to MWCNTs. The low content of this type of carbon will generate only a small perturbation in the properties of the supramolecular arrangement. Also, the oxidation potential of the TCh at the surface of MWCNT–TCNQ modified electrode (+150 mV) is clearly lower than the oxidation potential observed for MWCNT modified electrode (+300 mV). No response of TCh could be recorded for the bare SPE at +150 mV (see Fig. 3A). That shows that amorphous carbon has no influence on the electrochemical behavior of the electrode.

The effect of pH on the oxidation peak of TCh was investigated using a solution of TCh 5 mM. In the range of pH between 5 and 9 no significant changes of the peak potential were observed. It was concluded that the pH does not affect the sensor response in the working range around pH 8.

3.3. Amperometric measurements

Chronoamperometric experiments on MWCNTs–TCNQ/SPE were performed with different TCh concentrations (1, 2 and 5 mM) in PBS by polarizing the working electrode at +150 mV *vs.* pseudo-reference Ag electrode and the recorded chronoamperograms are presented in Fig. 4A. The catalytic rate constant and diffusion coefficient were calculated for two types of electrodes with and without Nafion membrane.

The equation:

$$\frac{i_{cat}}{i_{buffer}} = \pi^{1/2}(k_{cat}\, C\, t)^{1/2} \tag{3}$$

was used to calculate the catalytic rate constant k_{cat}, where i_{cat} and i_{buffer} are the currents in the presence and in the absence of TCh, C represents the TCh concentration and t is the time in second. The plot i_{cat}/i_{buffer} *vs.* $t^{1/2}$ for TCh 5 mM showed a linear dependence and the rate constant was calculated from the slope (inset, Fig. 4A). The value calculated for the electrode without Nafion was 3402 L mol^{-1} s^{-1} whilst for the electrode covered with Nafion the rate constant was 167 L mol^{-1} s^{-1}. The higher value represents a higher catalytic rate constant compared with other mediator modified sensor [7] That reveals the fact that the MWCNTs–TCNQ presents excellent electrocatalytical properties toward thiocholine oxidation. However, comparing with ionic liquid-CNTs modified sensors this value is smaller [10]. Despite the fact that Nafion stabilizes the electrode surface, it represents a barrier for TCh diffusion and consequently it was not used for further development of the pesticide biosensor.

Chronoamperometric measurements were done to estimate the thiocholine diffusion coefficient (D) based on Cottrel equation [10]:

$$i = \frac{nFAD^{1/2}C}{\pi^{1/2}t^{1/2}} \tag{4}$$

The linear parts of the plots of *i vs.* $t^{-1/2}$ (Fig. 4B) were used to calculate the slope for each TCh concentration. The diffusion coefficient of 4.8×10^{-7} cm^2 s^{-1} was determined from the plot $(I \times t^{1/2})$ *vs.* C_{Tch} for the electrode without Nafion, while a value of 6×10^{-8} cm^2 s^{-1} was determined for the electrode with Nafion. These results confirm the fact that the presence of the Nafion membrane represents a barrier for the analyte.

A typical calibration curve was obtained for MWCNTs–TCNQ/SPE and Nafion by successive additions of TCh in the concentration range between 0.05 and 10 mM TCh. A linear response was recorded in the range 0.05–0.6 mM TCh with a sensitivity of 45 µA mM^{-1} cm^{-2} and a detection limit of 28 µM. A slightly higher detection limit and a narrower linear range for TCh were achieved with a system based on SPE modified with SWCNTs functionalized with cobalt phtalocyanine [26].

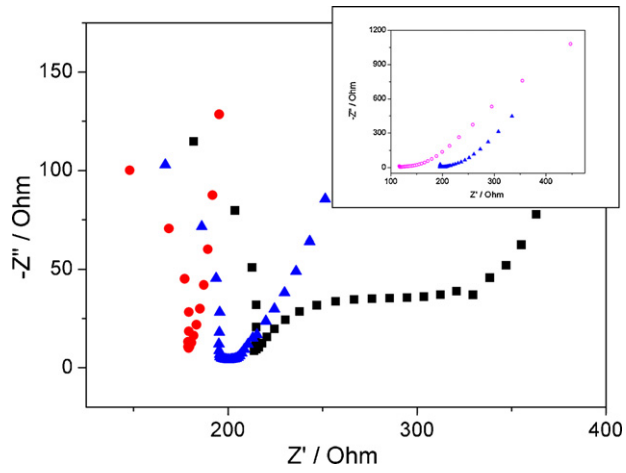

Fig. 5. Nyquist plots for the MWCNTs/SPE (●), TCNQ/SPE (■) and MWCNTs–TCNQ/SPE (▲) in the presence of 5 mM $Fe(CN)_6^{3-}/Fe(CN)_6^{4-}$ (frequency range 0.01 kHz–1 MHz, perturbation signal of 5 mV, OCP). Inset: Nyquist plots MWCNTs–TCNQ/SPE with (○) and without (▲) Nafion.

3.4. Electrochemical impedance spectroscopy characterization

The electrochemical properties of the MWCNTs–TCNQ were also tested using the EIS technique. A negatively charged redox couple $Fe(CN)_6^{3-}/Fe(CN)_6^{4-}$ was used, corresponding to the charge of thiocholine in the experimental condition (pH = 8). The electron-transfer resistance (noted R_{et}) is a parameter that depends on the dielectric and insulating properties at the interface. Its value gives information about the electron transfer kinetic at the interface electrode/electrolyte solution. Fig. 5 shows the Nyquist plots of the couple $Fe(CN)_6^{3-}/Fe(CN)_6^{4-}$ at the TCNQ/SPE (a), MWCNTs/SPE (b) and MWCNTs–TCNQ (c) electrodes. The plot reveals a semicircular part at high frequencies and a linear part at low frequencies. The first part corresponds to an electron transfer process and the second one to a diffusion process. The Randles circuit was chosen to fit the impedance data plots. No significant differences in R_{et} values were observed among three types of electrodes as follow: $214 \pm 3\ \Omega$ for TCNQ/SPE, $268 \pm 4\ \Omega$ for MWCNTs/SPE and $238 \pm 3\ \Omega$ in the case of MWCNTs–TCNQ/SPE (each value represents the mean for 3 replicates). A different behavior is observed at lower frequencies where TCNQ/SPE showed a significant increase of the impedance, while MWCNTs, due to its high conductivity and active surface, favors the electrochemical process. The MWCNTs–TCNQ exhibits properties that lie between the two components: TCNQ and MWCNTs. The active surface of the MWCNTs–TCNQ is probably smaller due to the formation of the supramolecular structure, determined by the TCNQ "bridges". Despite the high conductivity of the TCNQ molecules, they partially block the MWCNTs surface and hinder the interaction with the electrochemical mediator.

The insert of Fig. 5 shows a comparison between the Nyquist plots for SPEs modified with the MWCNTs–TCNQ in the presence and in the absence of Nafion. For the interpretation of the impedance spectra in the low frequency range, the diffusion of the redox probes has to be considered. The presence of Nafion as a protective layer for the immobilization of the MWCNTs–TCNQ has a negative effect on the electrochemical process. Due to the presence of negatively charged sulfonic groups, it does not favor the interaction of the electrode with negatively charged species like $Fe(CN)_6^{3-}/Fe(CN)_6^{4-}$ or TCh (pH = 8). Moreover, $Fe(CN)_6^{3-}/Fe(CN)_6^{4-}$ are very large ions and the diffusion process becomes limitative. EIS and chronamperometric studies converge to the conclusion that a higher sensitivity toward TCh will be obtained without Nafion.

3.5. Biosensor calibration for ATCh

The easiest way to immobilize AChE is to mix it directly with the MWCNTs–TCNQ and finally to depose the mixture on the electrode surface with or without Nafion. The fact that the carbon materials could partially adsorb the enzyme and the reactivator cannot reach the enzyme catalytic site is a main disadvantage of this approach. A full recovery of the AChE activity could not be achieved in these conditions, especially for a large reactivator molecule such as obidoxime. The deposition of the biocatalytical layer based on AChE in sol–gel was considered to stabilize the electrode surface. Taking into consideration the negative effect of Nafion proven by our previous EIS and chronoamperometric measurements, the construction of the biosensor was realized on the MWCNTs–TCNQ modified electrodes without Nafion. The good stability of the biosensor response makes us conclude that the sol–gel matrix prevents the loss of the MWCNTs–TCNQ from the electrode surface and the use of Nafion was not considered necessary anymore.

The enzymatic hydrolysis of ATCh was studied by amperometric measurements at a working potential of +150 mV by successive additions of ATCh in PBS. The thiocholine sensors were tested at concentrations in the range 0.1–10 mM ATCh. A very fast response of 15 s was observed, which indicates the absence of any diffusional limitation toward the enzymatic reaction. A typical Michaelis–Menten process is confirmed by the linear increase of the amperometric response until 8 mM ATCh and then reaching a plateau. Pesticide detection is performed by determining the enzyme activity before and after incubation with the inhibitor. To determine the enzyme activity, an excess of substrate is necessary in order to ensure a saturation of the enzyme catalytic sites. A concentration of 10 mM ATCh, which ensures enzyme saturation with substrate, was taken into consideration for further development of the pesticide biosensor. Reproducibility of analytical signal recorded in the presence of 10 mM ATCh was tested with 5 different biosensors from the same batch. A good reproducibility (RSD%), equal to 6% was obtained. Biosensors were stored at 4 °C in a buffer solution in order to preserve the enzyme activity immobilized in sol–gel matrix [11]. The signal reaches 96% from the initial value after 1 week, indicating a good stability of the AChE biosensor.

3.6. AChE biosensor. Proof of the concept

Paraoxon-methyl and chlorpyrifos were used as reference inhibitors for biosensor testing. Both are organo-phosphorous pesticides, paraoxon-methyl being recognized as a strong inhibitor, while chlorpyrifos as a weak one. Inhibition experiments on paraoxon-methyl 10^{-9} M were performed in order to optimize the incubation time (5–30 min). The inhibition degree increases with the incubation time from 15% to 64%. Paraoxon-methyl is a strong AChE inhibitor and for a longer incubation time, a permanent enzyme inhibition may occur by a dealkylation reaction (so called "aging" process). This affects the regeneration process and the ability of the biosensor to be reused. A longer inhibition time could be used only in the case of disposable AChE biosensors if it really brings an improvement of the sensitivity and a decrease of the detection limit. A shorter inhibition time is a requirement for a fast analysis of the pesticides. The calibration curves of paraoxon-methyl and chlorpyrifos were obtained after a 30 min incubation period. For each concentration, 5 replicates were obtained and the mean value of the inhibition degree was represented against the pesticide concentration. The calibration curves were linearized using a semi-logarithmic representation. The results are shown in Table 1.

The relative standard deviation of intra-assay and inter-assay were found to be 3.2% and 2.5%, respectively, in the case of

Table 1
Pesticide detection with AChE biosensors based on MWCNT–TCNQ/SPE; $I\% = a + b \times \log C_{pesticide}$ (M) (incubation time = 30 min).

Pesticide	*a*	*b*	*R*	Conc. range (nM)	LOD[a]	
					pM	ppt
Paraoxon-methyl	195 ± 12	17.6 ± 1.3	0.9722	0.1–500	30	7
Chlorpyrifos	258.2 ± 5.6	26.50 ± 0.70	0.9958	1–100	430	100

[a] $I = 10\%$.

Table 2
Real samples analysis: spiked tap water.

Pesticide	Pesticide added (nM)	Inhibition degree (%)		Recovery[b] (%)
		Standard solution	Spiked tap water[a]	
Paraoxon-methyl	1	37	36 ± 4	97.3
	10	55	52 ± 5	94.5
	50	67	64 ± 2	95.5
Chlorpyrifos	5	38	33 ± 2	86.8
	10	46	42 ± 4	91.3
	50	65	61 ± 3	93.8

[a] $n = 3$.
[b] Calculated for the mean value of the inhibition degree of the spiked samples.

paraoxon-methyl 10^{-1} M ($n = 5$) indicating a good reproducibility. Values of 3.5% and 3% were found for intra-assay and inter-assay RSD, respectively in the case of chlorpyrifos 10^{-9} M ($n = 5$).

The detection limit was calculated to be 30 pM (7 ppt) for paraoxon-methyl and 0.4 nM (0.1 ppb) for chlorpyrifos for an inhibition degree of 10%. This is one of the lowest detection limits reported for paraoxon-methyl using electrochemical biosensors based on commercial AChE taking into account that usually LOD of about ppb are reported [24,27]. Other biosensors based on SPEs modified with MWCNTs showed a LOD of 0.15 ppb for the same incubation period of 30 min [28], while the use of CNTs in combination with AChE entrapped in polyelectrolyte multilayers made possible a LOD of only 0.1 ppb paraoxon [8]. There are also other biosensors that have reported LOD lower than ppt, but these are either multi-layers and bi-enzyme systems [29] or are based on affinity interaction and piezoelectric detection [30].

The detection limit for chlorpyrifos achieved by us is similar to others reported in the literature [31,32]. Regeneration of the biosensor was realized with obidoxime as previously reported [11]. An optimization of the regeneration time and concentration was performed in the conditions of a relatively high incubation time with pesticide and use of a stronger AChE inhibitor-paraoxon-methyl. An incubation time of 15 min with obidoxime 5 mM was considered optimal to achieve complete regeneration for all range of concentrations of tested pesticide. In this sense, after the inhibition measurement, the biosensor was immediately immersed into the obidoxime solution and, after 15 min, washed twice with ultrapure water and finally with a buffer solution. This is necessary because traces of obidoxime in the sol–gel layer could have undesirable effects for further measurements [11]. The reproducibility of the inhibition was tested on paraoxon-methyl 10^{-9} M and chlorpyrifos 10^{-8} M. For 5 successive inhibition–regeneration cycles on the same biosensors, a reproducibility of 7% was achieved for paraoxon-methyl and 10% for chlorpyrifos, respectively, showing a good reproducibility of the inhibition determination.

Spiked samples of tap water were analyzed in order to test the biosensor accuracy. Tap water sample analysis leads to an inhibition degree below the detection limit (3.4%). Further, the inhibition tests were performed in standard pesticide solutions and by adding different amounts of paraoxon-methyl and chlorpyrifos in tap water samples. Spiked water samples with paraoxon-methyl concentrations of 1, 10 and 50 nM, respectively with chlorpyrifos 5, 10 and 50 nM were analyzed.

Experimental results presented in Table 2 show the inhibition degree for spiked samples and standard solutions. The inhibition degrees were in good correlation with those produced by standard solutions and indicated a good accuracy of the biosensor. The percentage of the recovery calculated as the ratio between inhibition degree of spiked sample and standard solution, respectively was smaller than 100% for both pesticides.

4. Conclusions

The proposed work illustrated that TCNQ and MWCNTs can interact in different ways and form supramolecular arrangements with enhanced electrochemical properties which were exploited in biosensors development. The DR-UV–vis and Raman spectroscopy studies allowed us to propose two different arrangements depending on the amount of TCNQ and to predict the electrochemical behavior of the MWCNT–TCNQ modified sensors. From the two proposed supramolecular arrangements, only MWCNT–TCNQ (1 mM)/SPE led to a sensitive, stable and reproducible response of the TCh sensor. Enhanced electrocatalytical activity of the MWCNTs–TCNQ is related to the distribution of TCNQ molecules between or along the CNTs and/or additional electrostatic interactions that stabilize the mediator in the MWCNT–TCNQ [16].

The lower mechanical stability of the modified SPEs was improved by the use of Nafion just for the characterization of the TCh sensor. Nafion stabilizes the surface of the electrode and minimizes the loss of the MWCNT–TCNQ from the electrode surface but has a negative effect on the electrocatalytical properties toward TCh. A better sensitivity and a larger linear range for thiocholine was achieved compared with a system based on covalent attachment of the mediator (CoPC) on the surface of SWCNTs [26]. The newly proposed concept represents a simple and reliable way to develop a highly sensitive and stable biosensor for detection of AChE inhibitors based on MWCNTs–TCNQ modified SPE. TCNQ as well as MWCNTs were previously used separately for these types of biosensors but this is the first report about the use of MWCNTs–TCNQ to decrease the overpotential of thiocholine oxidation and to monitor the AChE activity.

Although the length of the MWCNTs is different, TCNQ acts as a linker for MWCNTs generating supramolecular arrangements and also diminishes the effects that can be generated by individual entities. The nanotubes length had little relevance toward supramolecular arrangement from Fig. 2A compared with the outer

diameter of the nanotubes, for a given mass loading, since the interactions between TCNQ and MWCNTs are realized on the outer surface of the CNTs. Moreover, sonication of the MWCNT with TCNQ solution is expected to lead to the cutting of the MWCNTs into shorter fragments thus reducing the differences in the length of the MWCNTs [33].

The immobilization of AChE in sol–gel proved to offer a much lower detection limit for paraoxon-methyl (7 ppt) compared with covalent immobilization of the enzyme on the surface of CoPC-SWCNTs/SPE (3 ppb paraoxon) [27]. A fast response, high sensitivity toward pesticides and efficient reactivation of the enzyme by obidoxime was achieved with the developed system. Usually, the use of SPEs are related with the development of disposable biosensors, but in our case, the AChE biosensor can be successfully used up to 10 times due to its very good reproducibility. The analysis of the spiked tap water samples confirms the potential of the AChE biosensor to be used as screening method for sensitive detection of organophosphate and carbamate insecticides.

In comparison with other AChE biosensors based on CNTs and/or mediators, the proposed biosensor based on a MWCNTs–TCNQ exhibited very high sensitivity, a good reproducibility and stability. The biosensor construction is very simple and it represents a very affordable tool for the analysis of AChE inhibitors such as pesticides, drugs, micotoxins with a broad range of applications in food, environmental and clinical monitoring.

Acknowledgments

This work was supported by a grant of the Romanian National Authority for Scientific Research, projects PN-II-ID-PCE-2011-3-0286 and code 2125/2008. L.-G. Zamfir is grateful to the grant POSDRU 107/1.5/S/80765 for the doctoral fellowship. We would like to thank Dr. Bogdan Cojocaru for the DR-UV–vis, Raman spectra and elemental analysis.

References

[1] M. LeDoux, J. Chromatogr. A 1218 (2011) 1021–1036.
[2] A. Amine, H. Mohammadi, I. Bourais, G. Palleschi, Biosens. Bioelectron. 21 (2006) 1405–1423.
[3] S. Andreescu, J.-L. Marty, Biomol. Eng. 23 (2006) 1–15.
[4] D.M. Ivnitskii, J. Rishpon, Biosens. Bioelectron. 9 (1994) 569–576.
[5] J.P. Hart, I.C. Hartley, Analyst 119 (1994) 259–263.
[6] X. Sun, X. Wang, Biosens. Bioelectron. 25 (2010) 2611–2614.
[7] F. Arduini, A. Cassisi, A. Amine, F. Ricci, D. Moscone, G. Palleschi, J. Electroanal. Chem. 626 (2009) 66–74.
[8] G. Liu, Y. Lin, Anal. Chem. 78 (2006) 835–843.
[9] A. Merkoci, M. Pumera, X. Llopis, B. Perez, M. del Valle, S. Alegret, TrAC: Trends Anal. Chem. 24 (2005) 826–838.
[10] L. Rotariu, L.-G. Zamfir, C. Bala, Sens. Actuators B 150 (2010) 73–79.
[11] L.-G. Zamfir, L. Rotariu, C. Bala, Biosens. Bioelectron. 26 (2011) 3692–3695.
[12] R. Yuge, M. Yudasaka, A. Maigne, M. Tomonari, J. Miyawaki, Y. Kubo, H. Imai, T. Ichihashi, S. Iijima, J. Phys. Chem. C 112 (2008) 5416–5422.
[13] S. Andreescu, L. Barthelmebs, J.L. Marty, Anal. Chim. Acta 464 (2002) 171–180.
[14] A. Ivanov, G. Evtugyn, H. Budnikov, F. Ricci, D. Moscone, G. Palleschi, Anal. Bioanal. Chem. 377 (2003) 624–631.
[15] D. Martorell, F. Céspedes, E. Martínez-Fàbregas, S. Alegret, Anal. Chim. Acta 337 (1997) 305–313.
[16] J. Oh, S. Roh, W. Yi, H. Lee, J. Yoo, J. Vac. Sci. Technol. B 22 (2004) 1416–1419.
[17] R.G.A. Veiga, R.H. Miwa, Phys. Rev. B 73 (2006).
[18] J.P. McNamara, R. Sharma, M.A. Vincent, I.H. Hillier, C.A. Morgado, Phys. Chem. Chem. Phys. 10 (2008) 128–135.
[19] S.U. Lee, R.V. Belosludov, H. Mizuseki, Y. Kawazoe, Nanoscale 3 (2011) 1773–1779.
[20] C. Bonnet, S. Andreescu, J.-L. Marty, Anal. Chim. Acta 481 (2003) 209–211.
[21] D. Du, X. Huang, J. Cai, A. Zhang, Sens. Actuators B 127 (2007) 531–535.
[22] D. Du, X. Ye, J. Cai, J. Liu, A. Zhang, Biosens. Bioelectron. 25 (2010) 2503–2508.
[23] D. Du, J. Cai, D.D. Song, A.D. Zhang, J. Appl. Electrochem. 37 (2007) 893–898.
[24] F. Arduini, F. Ricci, C.S. Tuta, D. Moscone, A. Amine, G. Palleschi, Anal. Chim. Acta 580 (2006) 155–162.
[25] G.C. Hochberg, Polym. Int. 38 (1995) 119–124.
[26] E. Jubete, K. Zelechowska, O.A. Loaiza, P.J. Lamas, E. Ochoteco, K.D. Farmer, K.P. Roberts, J.F. Biernat, Electrochim. Acta 56 (2011) 3988–3995.
[27] A.N. Ivanov, R.R. Younusov, G.A. Evtugyn, F. Arduini, D. Moscone, G. Palleschi, Talanta 85 (2011) 216–221.
[28] K.A. Joshi, J. Tang, R. Haddon, J. Wang, W. Chen, A. Mulchandani, Electroanalysis 17 (2005) 54–58.
[29] W. Zhao, P.-Y. Ge, J.-J. Xu, H.-Y. Chen, Environ. Sci. Technol. 43 (2009) 6724–6729.
[30] J. Halámek, J. Přibyl, A. Makower, P. Skládal, F.W. Scheller, Anal. Bioanal. Chem. 382 (2005) 1904–1911.
[31] A. Hildebrandt, J. Ribas, R. Bragós, J.-L. Marty, M. Tresànchez, S. Lacorte, Talanta 75 (2008) 1208–1213.
[32] N. Prabhakar, K. Arora, S.P. Singh, M.K. Pandey, H. Singh, B.D. Malhotra, Anal. Chim. Acta 589 (2007) 6–13.
[33] C.J. Kerr, Y.Y. Huang, J.E. Marshall, E.M. Terentjev, J. Appl. Phys. 109 (2011) 094109.